J Solid State Electrochem (2008) 12:1205–1218
DOI 10.1007/s10008-007-0473-3

REVIEW PAPER

Different strategies for functionalization of diamond surfaces

Sabine Szunerits · Rabah Boukherroub

Received: 19 October 2007 / Revised: 21 October 2007 / Accepted: 21 October 2007 / Published online: 4 December 2007

Abstract Functionalization of diamond surfaces holds considerable promise from both fundamental and applied research aspects. This review summarizes briefly the state of the art of chemical, photochemical and electrochemical strategies for the grafting of different organic functionalities on diamond. Depending on the sought-after application and the desired physical property of diamond, halogenated, aminated, carboxylated and oxidized diamond surfaces have been proposed. After a brief introduction, the review is primarily divided into two parts, presenting chemical functionalisation strategies used on oxygen-terminated diamond, followed by methods used for the formation of C–C, C–X and C–N bonds on hydrogen-terminated diamond.

Keywords Hydrogen-terminated diamond · Oxidized diamond · Surface functionalization · Biomolecule immobilization · Characterization

S. Szunerits (✉)
Laboratoire d'Electrochimie et de Physicochimie des Matériaux et des Interfaces (LEPMI), CNRS-INPG-UJF,
1130 Rue de la Piscine, BP 75,
38402 St. Martin d'Hères Cedex, France
e-mail: sabine.szunerits@lepmi.inpg.fr

R. Boukherroub
Insstitut de Recherche Interdisciplinaire (IRI), FRE CNRS 2963,
Institut d'Electronique, de Microélectronique et de Nanotechnologie (IEMN), UMR CNRS-8520, Cité Scientifique,
Avenue Poincaré-BP. 60069,
59652 Villeneuve d'Ascq, France

Introduction

Diamond, a well-known gemstone, is famous among scientists for its combination of exceptional physical and mechanical properties such as high thermal conductivity, chemical inertness, optical transparency (from UV to IR), high mechanical stability and corrosion resistance. Due to its indirect optical band gap of 5.47 eV, diamond belongs to the group of wide band gap semiconductors. It exhibits an insulating character in the undoped state and a semimetallic to metallic behavior upon doping. Its superior properties have triggered many research activities on device-oriented applications, and diamond is, nowadays, used in electronic industry as field emitters. Other applications based on diamond include chemical and biological sensors, DNA and protein chips, and electrodes for electrocatalytic reactions.

These developments would not have been possible without experimental and theoretical efforts towards obtaining a fundamental understanding of the synthesis of diamond. Optimization of the growth conditions of synthetic diamond during recent years allowed the controlled deposition of electronic-grade quality with atomically flat surfaces. For a long time, diamond surface was considered as chemically inert to most reagents and its chemical modification difficult, in contrast to many other semiconductor surfaces. There are however several important exceptions to the generally low reactivity of diamond. First, diamond surfaces can undergo a phase transformation to graphite [1–3], and the graphite is subsequently used as the basis for additional surface reactions. This may not be particularly useful when relying on properties specific to diamond. Second, a diamond surface can be oxidized. Yet, the most obvious oxidative method, heating diamond in the presence of O_2, forms graphite [4].

In the last 15 years, progress has been made in the development of easy, controllable and specific surface modification methods for the introduction of different functional groups on the diamond surface. These methods are based on chemical, photochemical, and in the case of doped diamond, electrochemical concepts. Depending on the sought-after application and the desired physical property of diamond, halogenated, aminated, carboxylated and oxidized diamond surfaces have been prepared. While the interest in fluorinated diamond films comes, for example, from its improved friction properties and water repulsion behavior comparable to poly(tetrafluoroethylene) [5], aminated diamond surfaces have allowed successfully grafting of oligonucleotides, peptides, proteins and gold nanoparticles onto diamond surface [6–10].

Because of the increased interest in the surface chemistry of diamond, this review is devoted to discuss, in more detail, some of the approaches employed by different groups to functionalize hydrogenated and oxidized diamond surfaces.

Fabrication of diamond substrates

Polycrystalline diamond films

The use of diamond has been facilitated since the beginning of the 1980s through the discovery and development of processes for large-scale production. It was discovered that polycrystalline diamond films (Fig. 1a) can be formed by chemical vapor deposition (CVD) techniques, which involve a chemical reaction occurring above a solid surface in the gas phase, causing deposition of the diamond onto that surface [11]. CVD is nowadays well established and well described in a number of review articles [12, 13]. In short, CVD techniques require, for producing diamond films, a means of activating gas-phase carbon-containing precursor molecules. The activation of gas phase molecules can be achieved by three different means: (1) thermally (e.g., hot filament), (2) via plasma activation (D.C., R.F., or microwave), (3) through the use of a combustion flame (oxyacetylene or plasma torches). While each method differs in its details, they all share common features during the growth process: temperatures in the range of T=1,000–1,400 K, and the gas precursor is diluted in an excess of hydrogen (typical CH_4 mixing ratio ~1–2 vol.%).

The fact that diamond films can be prepared by CVD techniques is linked to the presence of hydrogen atoms, which are generated as a result of the gas being activated either thermally or via electron bombardment. The hydrogen atoms are believed to play a number of crucial roles in the CVD process: they undergo hydrogen abstraction reactions with stable gas-phase hydrocarbon molecules, producing highly-reactive carbon-containing radical species. This is important, as stable hydrocarbon molecules do not react to cause diamond growth. These reactive radicals, especially methyl radicals, can diffuse to the substrate surface and react, forming the C–C bond necessary to propagate the diamond lattice. Even though atomic hydrogen etches diamond under typical CVD conditions, the rate of diamond growth exceeds its etch rate. For other forms of carbon (graphite, glassy carbon, etc.) the converse is true, and this is therefore believed to be the basis for the preferential deposition of diamond rather than graphite. Nonetheless, the morphology and quality of the resulting diamond films depends on the precise growth conditions. One of the challenges faced by the researchers in CVD diamond technology was to increase the growth rates to economically viable rates (such as 1 mm h^{-1}) without compromising film quality. High growth rates could be only achieved at the expense of a corresponding loss of film quality, where high film quality implies that the ratio of sp^3 (diamond) to sp^2-bonded (graphite) carbon in the sample is high, the C–C vs C–H bond content is enhanced and that the film is crystalline. Progress has been made using microwave deposition reactors, as the deposition rate has been found to scale approximately linearly with applied microwave power.

Nanocrystalline and ultrananocrystalline diamond films and powders

The use of CVD techniques for diamond film formation is often hampered by the polycrystalline nature of the films. The numerous grain boundaries and crystal defects in

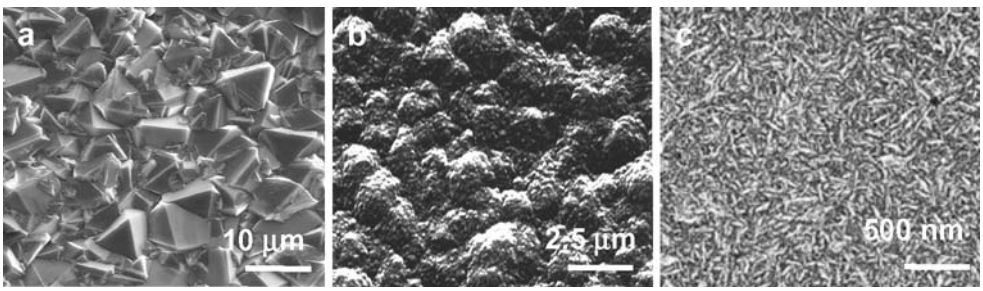

Fig. 1 SEM images of (**a**) polycrystalline diamond, (**b**) nanocrystalline diamond and (**c**) ultrananocrystalline diamond thin films

polycrystalline diamond reduce electron and hole motilities and degrade the electronic performance of diamond. The diamond film morphology depends on the reactant gases, their mixing ratios and the substrate temperature. At low partial methane pressure, highly crystalline diamond films are obtained. The crystalline morphology disappears with increasing pressure, forming diamond films with amorphous structure resembling more disordered graphite containing small clusters of diamond nanocrystals. Growing at specific conditions between these two extremes can yield high quality (mostly sp^3) nanocrystalline and ultrananocrystalline diamond films, which possess a much smoother surface and enhanced electronic properties (Fig. 1b,c). A number of synthetic methods for the preparation of nanocrystalline diamond (ND) and ultrananocrystalline (UNCD) diamond in the form of films and powders have been developed [14–19]. UNCD film consists of diamond grains of predominantly 3–5 nm in size in an amount of no less than 10^{10} atoms cm^{-3} with abrupt grain boundaries, consisting of a mixture of sp^3- and sp^2-bonded carbons. Thin UNCD films, synthesized using microwave plasma chemical vapor deposition with argon-rich Ar/CH_4 plasmas, exhibit similar physical, mechanical and electrochemical properties as microcrystalline diamond [20–22]. UNCD can be made into very highly n-type, room-temperature conductive via the addition of nitrogen gas to the plasma, yielding films with room temperature conductivities as high as 250 Ω^{-1} cm^{-1}[23]. Microwave-plasma-enhanced CVD was used also to form single-crystalline diamond with atomically smooth surfaces [24–26].

Physical characteristics of hydrogen-terminated diamond

Although diamond is composed of only carbon atoms, the diamond surface is stabilized by bonding to elements rather than carbon, as grown diamond films can be considered as being hydrogen terminated (H-terminated). Undoped H-terminated diamond shows insulating behavior in vacuum but p-type surface conductivity when exposed to air [27]. This contrasts to oxygenated diamond (O-terminated), which is, in its natural state, electrical, insulating in vacuum and in air. It is certain that the conductivity is related to hydrogen content. Several controversial models have been proposed to explain this induced p-type surface conductivity (which is still not well understood) such as (1) surface band bending due to valence-band electron transfer into an adsorbate layer (transfer doping model) [28–30], (2) hydrogen-introduced surface acceptors [31] and (3) deep-level passivation by hydrogen [32].

The high electrical resistivity (typically$>10^8$ Ω cm) of undoped diamond can be lowered through doping, replacing the semiconductor behavior by a semimetallic or metallic one depending on the doping level. Boron doping resulting in a p-type semiconductor can be achieved during the synthesis of diamond by addition of diborane gas [33]. While p-type diamond films are already available with good quality, the question of finding a shallow n-type dopant for diamond is still open [34–36]. Heavily boron-doped diamond (BDD) films ($N_A>3\times10^{20}$ B cm^{-2}) have gained rapidly interest since its first report as a novel electrode. Through the study of the electrolysis of aqueous H_2SO_4 solutions, the large potential window of water stability has been pointed out [37]. The wide electrochemical potential window of O-terminated diamond together with small background current in aqueous media helped the development of a large range of electroanalytical applications of BDD interfaces [38]. The fluorinated diamond (F-terminated) displays, so far, the widest range of potentials (5 V polarization window) for an electrode material in aqueous solution, being limited only by the formation of free hydrogen [E^0 (H^+/H_2)=−2.3 V_{SHE}] and hydroxyl [E^0 (OH^-,H^+/H_2O)=2.74 V_{SHE}] radicals [39, 40]. These electrodes were formed through radio-frequency-based plasma fluorination [41]. It was found that three-quarters of the sites on (111) surface could be fluorinated. On the other hand, on the (100) surface, less than half of the surface sites are fluorinated and low-energy electron diffraction showed no ordered surface structure [42]. This is consistent with the theoretical estimation of Harrison and Belton, who showed appreciable steric hindrance of C–F on diamond (100) and much less on (111) [43].

The way diamond surface is stabilized, H-terminated or O-terminated, has additional physical and chemical effects. Besides the differences in electrical conductivity, it includes the change of wetting properties: hydrophobic for a H-terminated and hydrophilic for an O-terminated diamond film, and the difference in electron affinity: negative electron affinity for H-terminated and positive electron affinity for O-terminated diamond. These differences in electron affinity are mainly caused by the surface dipole difference between C–H and C–O bonds [44] and has important consequences for the kind of surface chemistry that can be successfully performed on diamond films. There might be still additional advantages of diamond electrodes over conventional electrodes which are not yet realized.

Cyclic voltammetry (CV) on doped diamond has proven to be a powerful method to distinguish between the surface states of diamond with the same doping level [45, 46]. This difference is possible, as the heterogeneous electron transfer reaction of several redox mediators at the BDD interface is mediator dependent. Broadly, one can distinguish between two types of redox mediator: outer sphere (e.g., $Ru(NH_3)^{3+/2+}$, $IrCl_6^{2-/3-}$, $Ru(bpy)_3^{3+/2+}$) and inner sphere [$Fe(CN)_6^{3-/4-}$, $Fe^{3+/2+}$] electron transfer

Table 1 Conditions for electrochemical oxidation of H-terminated diamond

Solution	Potential	Conditions	Reference
1 M $HClO_4$	Potentiostatic at +3 V/SCE	20 min	[60]
Phosphate buffer	Cycling between 0 and 2.5 V/SCE	7 scans	[53]
3 M H_2SO_4	Cycling between −0.5 and −2.5 V/RHE	Several scans	[61]
0.5 M H_2SO_4	Potentiostatic at +3 V/SCE	30 min	[62]
0.1 M KOH	Potentiostatic at 2.6 V/Ag/AgCl	60 min	[63]
0.2 M $NaSO_4$	Potentiostatic at 2.2 V/SCE	3 min	[52, 64]

mediators. The characteristics of outer sphere electron transfer mediators are that the electron kinetics for this type of reaction are relatively insensitive to factors such as surface termination and microstructure, but very sensitive to the density of electronic states near the formal potential. Apparent rate constants between 0.01 and 0.2 cm s^{-1} are commonly found for high-quality diamond electrodes. In the case of an inner-sphere electron transfer, the electrode kinetics is highly sensitive to the diamond termination as the reaction appears to proceed through a specific surface site. In the case of H-terminated and O-terminated diamond, the apparent rate constants are two orders of magnitude apart [47].

Oxidation of H-terminated diamond surfaces

Freshly synthesized H-terminated diamond interfaces can be left without special precautions on the bench for several months. In spite of the high stability of diamond, oxidation of the hydrogenated surface is relatively easy to perform. The resulting oxidized surface is so stable that it can be recovered only by hydrogen plasma treatment at elevated temperatures. Diverse procedures have been reported for the oxidation of H-terminated surfaces including thermal [48–50], plasma [51, 52] and electrochemical techniques [53–56, 65], as well as the use of singlet oxygen [53], irradiation with vacuum ultraviolet light (VUV, λ=172 nm, t=3 h in the presence of O_2 and H_2O) [57] and ozone treatment [58–60]. No real attempt has been made in the literature to compare these different approaches adequately, and no recommendation can be found regarding the best approach. Foord et al. have studied in more detail the difference in efficiency of the electrochemical activation and the oxygen low temperature plasma treatment. They found that oxygen plasma is probably the most efficient method for the oxidation of diamond surfaces [54]. However, the reported electrochemical approaches vary significantly (Table 1):

Independent of the activation method used, the presence of oxygen on the diamond surface has a significant influence on the chemical reactivity [55, 66], electrical conductivity [67, 68], field emission [69, 70] and Schottky barrier heights [71].

Figure 2 shows typical high resolution X-ray photoelectron spectra of a hydrogen-terminated and a photochemically oxidized boron-doped (BDD) polycrystalline diamond surface [58]. The XPS spectrum of the C 1s of a hydrogenated BDD sample displays a main peak at ~285 eV. The peak is unsymmetrical. The presence of a shoulder at higher binding energy (~286 eV) is most likely due to the presence of amorphous carbon at the grain boundaries. After photochemical oxidation, the XPS spectrum displays three different features: a peak at 285 eV due to C 1s from the bulk with a shoulder at 286 due to the surface C–O features further seen at 289 eV . Based on the diamond structure, it is expected that the sp^3 C–H bonds on the (111) facets will be terminated with hydroxyl groups, while the CH_2 bonds on the (100) facets will be transformed to carbonyl and

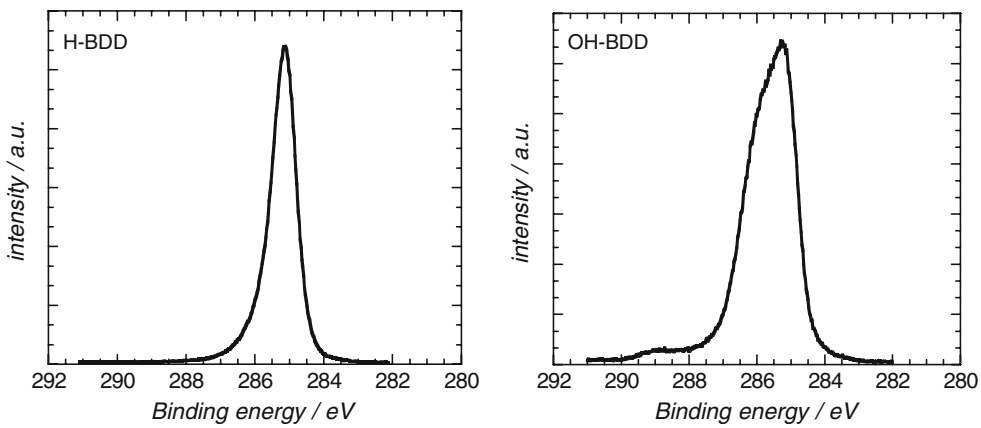

Fig. 2 High resolution XPS spectra of C 1s of hydrogenated and photochemically oxidized boron-doped diamond surfaces

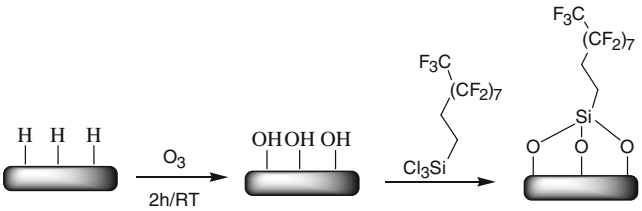

Fig. 3 Schematic illustration of the silanization reaction of oxidized diamond surface with perfluorodecyl trichlorosilane

ether functional groups. The signals from surface hydroxyl and ether groups are undistinguishable (~286 eV; 72, 73]). The peak at 289 eV results most likely from a contribution of carbonyl groups on the surface.

Chemical functionalization of oxygen-terminated diamond surfaces

Silanization

As silane reagents show no reactivity towards carbonyl or ether groups, they can be used to underline the presence of hydroxyl groups on oxidized diamond. Notsu et al. reacted electrochemically and oxygen plasma-oxidized boron-doped diamond surfaces with 3-aminopropyltriethoxysilane (APTES) and characterized the silanized interface using XPS and contact angle measurements [56, 73]. The authors have observed that the water contact angle decreased after surface oxidation (from 67.0 ° to 25.8°) and increased again to some extent after APTES treatment (43.4 °). The presence of a N 1s peak in the XPS spectrum of the modified surface indicates further the success of the silanization reaction. On the other hand, the presence of surface hydroxyl groups on photochemically oxidized diamond surfaces was confirmed by the chemical reaction

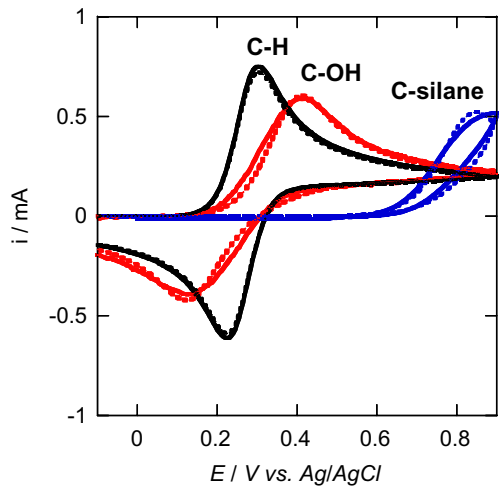

Fig. 4 Experimental (*bold lines*) and simulated (DigiSim 3.03, *dotted lines*) cyclic voltammetric *i–E* curves for hydrogenated, photochemically oxidized and silanized diamond electrode: solution: $Fe(CN)_6^{4-}$ (10 mM) in KCl (0.1 M)/water, scan rate=0.1 V s^{-1}, geometric area=0.283 cm^2

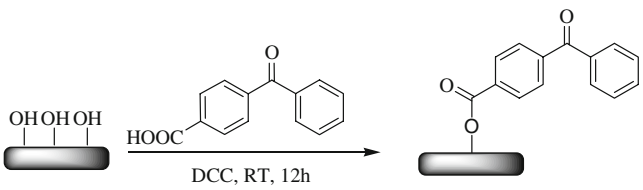

Fig. 5 Schematic illustration of the esterification reaction of hydroxylated diamond

of the oxidized BDD surface with perfluorodecyl trichlorosilane [CF_3–$(CF_2)_7$–CH_2–CH_2–$SiCl_3$] at room temperature (Fig. 3; [72]).

XPS analysis of the resulting surface showed the presence of peaks due to F 1s (687 eV), Si 2p (99 eV) and Si 2s (151 eV), consistent with the incorporation of an organic layer on the diamond surface. Furthermore, contact angle measurements agree well with a change of the wetting properties of the surface before and after silanization. Indeed, oxygen-terminated BDD surface displays a hydrophilic character with a water contact angle of 36°, while the perfluorodecyl-modified BDD is hydrophobic with a contact angle of 109°.

The barrier properties of oxidized and silanized diamond surfaces was investigated using cyclic voltammetry. Figure 4 shows the different electrochemical behaviors for H-BDD, oxidized and silanized BDD in the presence of $Fe(CN)_6^{4-/3-}$. The electron transfer kinetic is inhibited for the oxidized surface with an apparent rate constant of k^0_{app}=0.0005 cm s^{-1} (H-BDD: k^0_{app}=0.012 cm s^{-1}). The perfluorodecyl terminated diamond blocks effectively the surface, and a $k^0_{app}=8\times 10^{-8}$ cm s^{-1} was determined through modeling [72].

Recently, we also showed that *N*-(3-trimethoxysilylpropyl) pyrrole (TMPP) can be linked to oxidized BDD [74]. The functional silane layer allowed localized polymer formation to be achieved on the TMPP-modified BDD interface using the direct mode of a scanning electrochemical microscope (SECM) and an electrochemical scanning near-field optical microscope (E-SNOM). Depending on the method used,

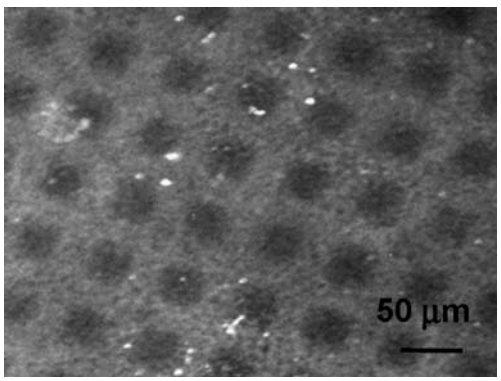

Fig. 6 Fluorescence images of photochemically linked GFP (t= 30 min, λ=350 nm, P=5 mWcm^{-2}) on a patterned BDD surface. The *bright lines* are coated with GFP molecules, while the *dark squares* correspond to oxidized regions

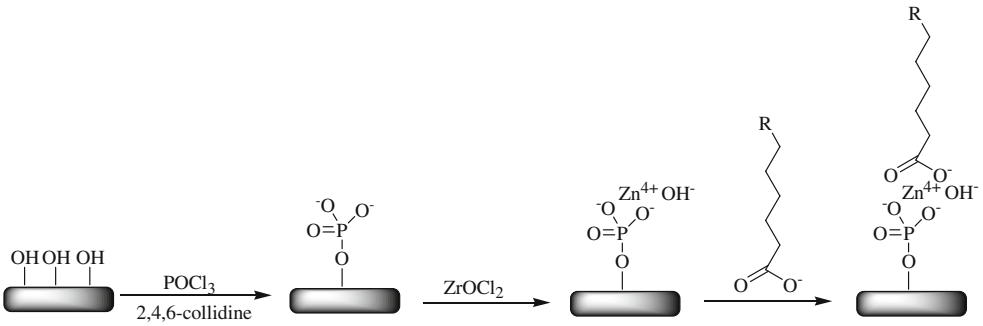

Fig. 7 Zirconium phosphate chemistry on oxidized diamond surface

polypyrrole dots with diameters in the range of 1–250 μm are electrogenerated.

Esterification

The hydroxyl groups of oxidized BDD were successfully tethered to organic molecules through an esterification reaction. Pyrene alkylcarboxylic acid, [75] biotin [53], and more recently, 3-benzoylbenzoic acid were covalently linked to oxidized diamond (Fig. 5; [76]).

To reveal the biotin grafting, the authors exploited the strong affinity of biotin to fluorescently labeled streptavidin. On the other hand, the photoelectrochemical behavior of a pyrene-terminated BDD surface was studied, and cathodic photocurrents have been measured in oxygen-saturated electrolyte.

The benzophenone terminated BDD surface was successfully used for photochemical immobilization of DNA, peptides and proteins. Benzophenone is as an efficient photoactivable group, stable under ambient light and protic solvents [77, 78]. Green fluorescence protein (GFP) was linked to benzophenone-modified BDD by exposing the surface to blue light (λ=350 nm) for 30 min. Figure 6 shows the fluorescence image of the covalently linked GFP on a patterned BDD surface.

Zirconium phosphate chemistry has recently been adapted to oxidized diamond (Fig. 7; [79]). Carboxylic acid layers can be bound to the diamond surface by coordination to zirconium phosphate functionalities. Pyrene was linked in this manner to BDD, and a surface coverage based on geometric surface area of 5×10^{-11} mol cm^{-2} was determined.

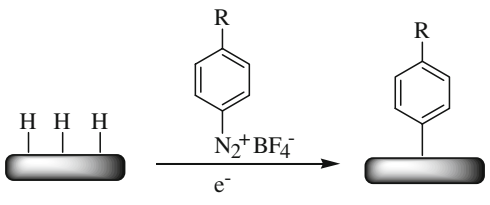

Fig. 8 Attachment of organic layers by reduction of aryl diazonium salts

Functionalisation of hydrogen-terminated diamond surfaces through C–C bond formation

Reduction of diazonium salts

One method available for the formation of a strong C–C bond between diamond and an organic molecule was first reported by McCreery and Swain [80] and consists of the electrochemical reduction of diazonium salts (Fig. 8; [17, 80–89]). Different diazonium salts are commercially available, but they can also easily be prepared in one step from a wide range of aromatic amines. The techniques offer the advantage of the availability of a wide range of functional groups (–COOH, X, NO_2, etc.) that can be introduced onto the surface in one step.

The method, intensively used for other carbon-based materials [90–100], is quite simple and can be performed in acetonitrile (CH_3CN + 0.1 M Bu_4BF_4) and acidic aqueous solutions (0.1 M H_2SO_4) through electrochemical reduction of diazonium salts. Covalent bonds between the diamond and the diazonium salt can, in addition, be formed through a spontaneous binding (in the absence of external bias) of the diazonium salt in the presence of 1% sodium dodecyl sulfate (SDS; [88], Shul, et al. 2007, submitted for publication). We recently showed that solvent-free functionalization of hydrogen-terminated boron-doped diamond surfaces with aryldiazonium salts using ionic liquids (1-butyl-3-methylimidazolium hexafluorophosphate or 1-butyl-3-methylimidazolium methyl sulphate) can be achieved in high yield (Shul, et al. 2007, submitted for publication). The electrons necessary for the reduction of the diazonium salt are, in these cases, most likely provided by the diamond itself [100]. This purely chemical grafting is attractive, as it does not require electrochemical equipment or doped diamond interfaces. The authors have also evidence from ellipsometric measurements that the chem-

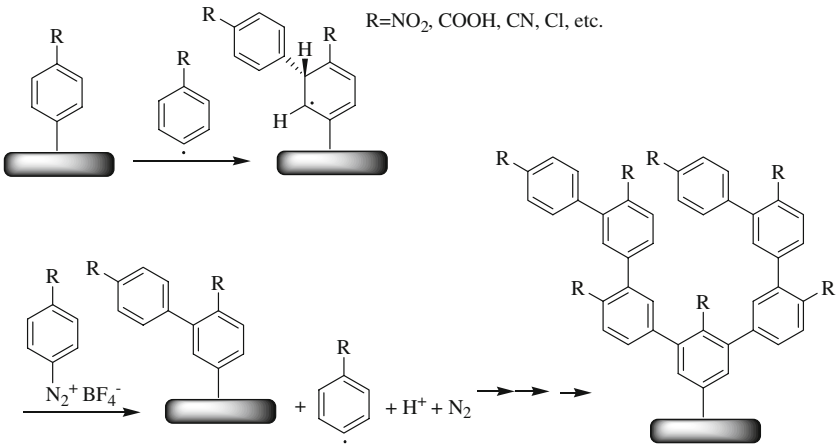

Fig. 9 Multilayer formation using diazonium salt reduction [99]

ical approach results more readily in monolayers rather than multilayers observed under electrochemical conditions. AFM measurements have evidenced the formation of multilayers using the electrochemical route, and the formation of a real monolayer was only reported on pyrolyzed photoresist [91]. Phenyl radical species are formed next to nitrogen during the grafting process, which react directly with the diamond surface. The formation of multilayers is due to an attack of the first grafted aryl group by another aryl radical (Fig. 9).

The principal interest in diazonium-based diamond modification is that the diamond-tethered functional groups are

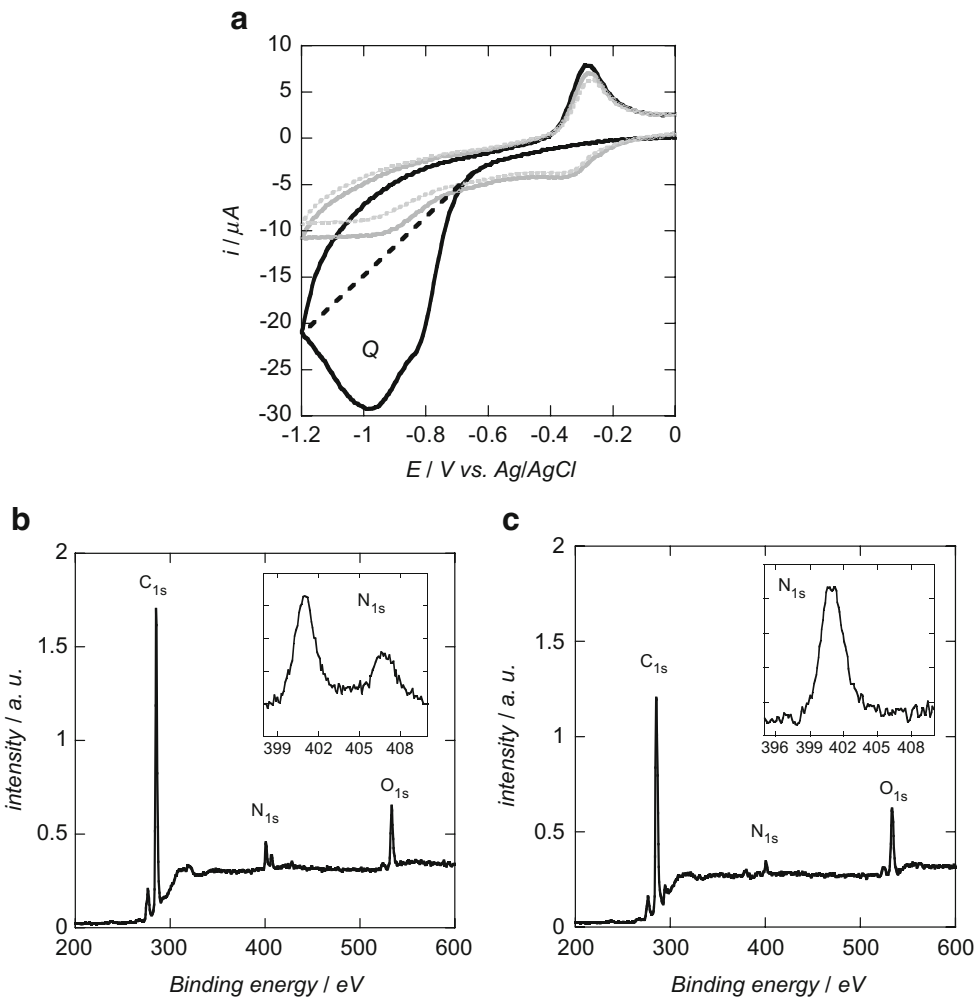

Fig. 10 a Cyclic voltammograms recorded in an aqueous (90%water/10%EtOH) 0.1 M KCl solution of a H-BDD modified with 4-nitrophenyl diazonium salt (1 h in SDS/water), scan rate=50 mV s^{-1}; XPS survey spectra of the BDD before (**b**) and after electrochemical reduction of NO_2 groups (**c**). The *insets* shows the high resolution XPS spectra of N 1s before (**b**) and after NO_2 reduction (**c**; Shul, et al. 2007, submitted for publication)

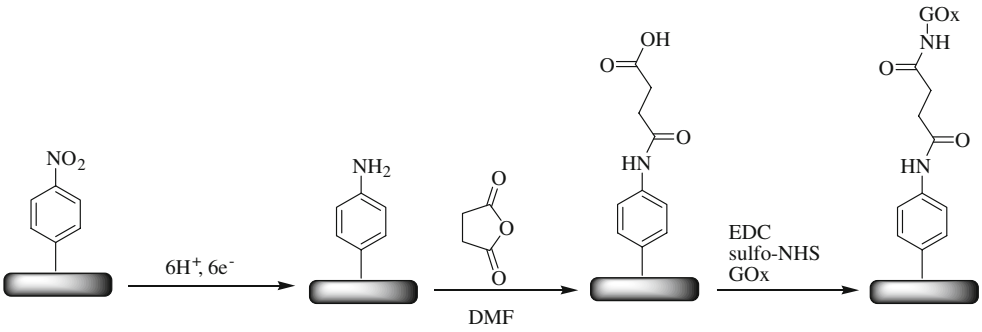

Fig. 11 Covalent immobilization of glucose oxidase on amine-terminated BDD surface

used for the covalent linking of biomolecules. This is due to the reported biocompatible and bio-inert character of diamond electrodes making them promising platforms for biosensing.

The most intensively studied diazonium salt derivative is the nitrophenyl salt. The key to biomolecular functionalization lies in the ability to selectively reduce nitro groups to primary amines to which DNA and other biomolecules can chemically be linked. In aqueous solution, an irreversible multi-electron and multi-proton reaction of the nitro group to amine (–NH_2) or hydroxyaminophenyl (–NHOH) groups takes place [101].

$$R - NO_2 + e^- \rightarrow R - NO_2^-$$
$$R - NO_2 + 4H^+ + 4e^- \rightarrow R - NHOH + H_2O$$
$$R - NHOH + 2H^+ + 2e^- \rightarrow R - NH_2 + H_2O$$

The reduction of the nitro group proceeds at potentials between −0.8 and 1.2 V and is mainly completed in the first cycle of the reduction step. Figure 10a shows the electrochemical reduction of a 4-nitroazobenzene (NAB)-modified polycrystalline BDD in aqueous solution to 4-aminoazobenzene-terminated BDD. XPS survey spectra (Fig. 10) recorded after five cycles show that all the –NO_2 groups have been converted into –NH_2 bonds. Indeed, after modification of the BDD surface with NAB molecule (Fig. 10b), additional peaks at 531, 401 and 407 eV due to O 1s, N 1s from –N=N and NO_2, respectively, were observed. The absence of a peak at ~402 eV from N 1s of the diazonium molecule is consistent with a covalent linking of the NAB molecules on the surface and not physisorption. The O 1s results most likely from the –NO_2 groups, but may also be due to partial oxidation and/or contamination of the surface. The XPS survey spectrum of the NAB-terminated BDD surface after electrochemical reduction (Fig. 10c) shows the disappearance of the component at 407 eV, in agreement with the reduction of –NO_2 to –NH_2 groups. However, the electrochemical reduction of the terminal nitro to NH_2 groups led only to a small decrease of the intensity of O 1s signal. This confirms that the O 1s peak observed in the XPS survey originates also from surface oxidation and/or contamination.

Integration of the cathodic peak using equation 1 (Q is the electrical charge passed during the electrochemical reduction of the nitro group, F is the Faraday constant, A the area of the electrode and n the number of electrons required for reducing a single nitro group) allowed determining the surface density:

$$\Gamma = \frac{Q}{nFA} \quad (1)$$

A surface density of 5.4×10^{-10} mol cm^{-2} was found in this particular case (Shul, et al. 2007, submitted for publication). Reported surface densities vary between 1.3×10^{-10} to 7.5×10^{-10} mol cm^{-2} [17, 82, 85, 89, 102, Shul, et al. 2007, submitted for publication]. A close-packed nitrophenyl layer on flat surfaces is reported to yield a density of 12×10^{-10} mol cm^{-2} [98].

The covalent linking of enzymes (glucose oxidase and tyrosinase) was achieved on the amine-terminated diamond

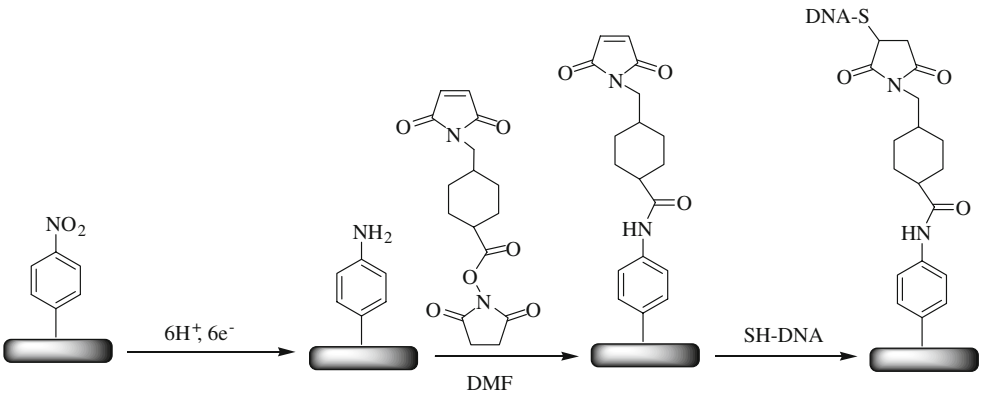

Fig. 12 Covalent linking of DNA using a heterobifunctional cross-linker (sulfo-succinimidyl 4-(*N*-maleimidomethyl) cyclohexan-1-carboxylate) to which thiol-modified DNA was linked

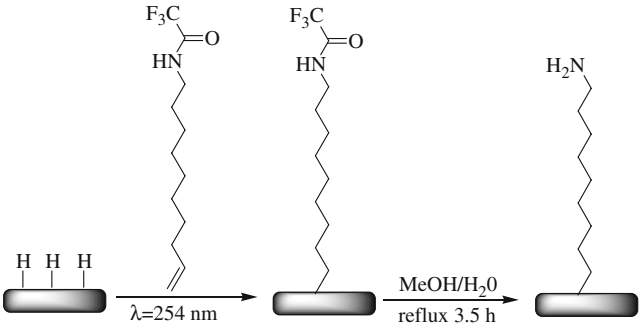

Fig. 13 Photochemical linking of organic molecules to H-terminated diamond

surfaces. Carlisle et al. [87] reacted the amine terminal groups on the BDD with succinic anhydride and *N*-hydroxysulfosuccinimide to link glucose oxidase (Fig. 11). Glucose was detected through the oxidation of biocatalytically formed H_2O_2. An amperometric biosensor for phenol, *p*-cresol and 4-chlorophenol was developed by Zhin et al. [89]. It is based on covalent immobilization of tyrosinase on amine-terminated BDD via carbodiimide coupling by forming an amide bond between the carboxylic acid of the tyrosine and the NH_2 of the BDD. They reported that 90% of the enzyme activity was retained for 5 weeks when storing the sensor at 4 °C in PBS.

On the other hand, DNA immobilization was achieved by immersing the amine-terminated diamond into a heterobifunctional cross-linker (sulfo-succinimidyl 4-(*N*-maleimidomethyl) cyclohexan-1-carboxylate) to which thiol-modified DNA was linked (Fig. 12) [84, 85, 88]. Experiments on single-crystalline diamond showed that the DNA chains are tilted by 31° with a DNA density of 6×10^{12} molecules cm^{-2}. The results are not affected by variation of the buffer salinity [84]. The structural and mechanical properties of a DNA double helix bonded to NH_2-terminated single crystalline diamond surfaces, prepared via photochemical or electrochemical routes, were evaluated using contact mode AFM. It was shown that DNA molecules can be irreversibly removed from the diamond surface by contact mode AFM with forces *N*>

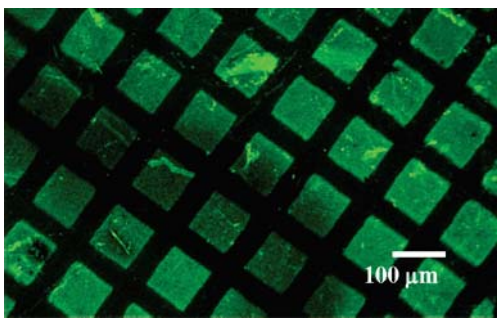

Fig. 14 Fluorescence images of patterned FITC-labeled DNA immobilized on diamond which has been biofunctionalized with undecylenic acid and subjected to repeated denaturation/rehybridization cycles (three cycles; reprint with permission from [112])

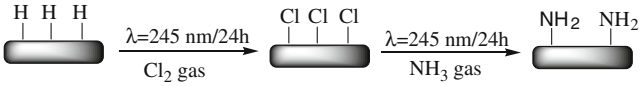

Fig. 15 Preparation of an amine-terminated BDD surface in a two-step procedure, consisting on the photochemical irradiation of a hydrogenated surface with chlorine followed with ammonia gas

45 nN and >76 nN on photochemically and electrochemically functionalized diamonds, respectively [86].

Covalent linking of anthraquinone diazonium salt to BDD through electrochemical reduction was recently shown by Foord [81]. In basic solution, the quinone-catalyzed reduction of oxygen was seen at −0.8 V/SCE.

Photochemical reaction with functional alkenes

H-terminated polycrystalline films exhibit a number of usual properties, including the ability to emit electrons from the valence band directly into a vacuum when illuminated with 254 nm light [103]. Ultraviolet irradiation of hydrogen-terminated diamond covered with liquid films of an appropriate alkene is an additional approach to produce functionalized diamond (Fig. 13). This scheme has been first proposed by Hamers et al. [102, 104–108] and is now used by different groups [24, 25, 109–112]. UV irradiation of hydrogen-terminated diamond surface in the presence of a liquid film of appropriate alkenes (e.g., 12-amino-dec-1-ene protected with a trifluoroacetic acid group, perfluorodecene, trifluoroethyl ester of ω-undecenoic acid, etc.) results in the formation of an organic layer covalently grafted to the surface through C–C bonds. While the stability of the formed monolayer has been proven [113–115], many questions remain about how the reaction proceeds mechanistically and how the organic film is organized on the surface. Hamers et al. carried out mechanistic and structural studies on photochemical functionalized diamond surfaces [116, 117]. They demonstrated that the modification process is not controlled by grain boundaries and that the functionalization is a surface-mediated reaction initiated by the photoejection of electrons from the diamond surface into the liquid phase [116].

Figure 13 displays the strategy used to incorporate terminal $–NH_2$ functional groups onto a diamond surface. To provide chemically reactive amine groups, the trifluoroacetamide protecting group was chemically removed, and DNA was linked to the amine-terminated diamond surfaces using a heterobifunctional cross-linker as discussed above. Comparing the DNA-modified diamond with a silicon surface modified in the similar way showed no loss of DNA over 15 hybridization/denaturation cycles on diamond and a loss of 1.8% on silicon [118]. The direct photochemical coupling using undecylenic acid was recently found to form a higher density of carboxylic acid groups on the diamond compared to trifluoroethylundecenoate

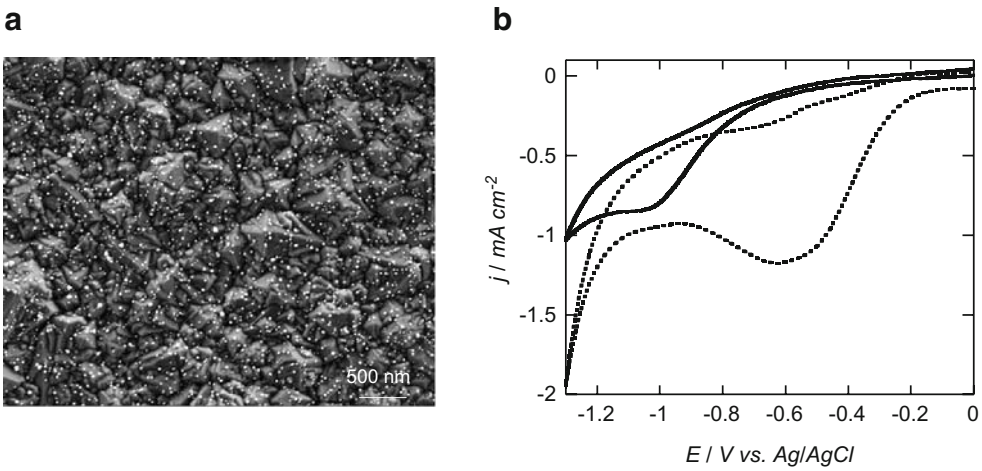

Fig. 16 **a** SEM image of polycrystalline aminated BDD exposed to a gold colloid solution, **b** Cyclic voltammograms of NH_2–BDD (*full line*) and NH_2–BDD/Au NP (*dotted line*) in aqueous solution of 0.1 M NaOH, scan rate: 100 mV s^{-1}

[112]. Figure 14 shows the fluorescence image of fluorescein isothiocyanate (FITC)-labeled DNA immobilized on acid-modified diamond and subjected to three denaturation–rehybridization cycles.

While the photochemical derivatization allows the introduction of several functional groups on the surface, the reaction time required is rather long (in the range of 12–15 h), and most of organic molecules absorb at the used wavelength. Nevertheless, glycol compounds could be linked to diamond allowing the study of nonspecific binding of proteins [109]. Electrochemical impedance spectroscopy (EIS) was used to characterize the modified interfaces and showed that the monolayer strongly inhibits electron transfer, but the detection of biological binding events in real time, as a consequence of the field effect induced in the diamond by the charged DNA, is possible [119]. EIS measurements, together with cyclic voltammetry, were performed on horseradish-peroxide-modified nanocrystalline diamond films [111]. The proximity of the haem groups to the diamond surface allowed direct electron transfer between them.

Functionalisation of hydrogen-terminated diamond surfaces through other bond formation

C–X bonds

A practical method for surface modification of diamond is the direct reaction with radical species in the gas phase. The radical moieties known to react directly with diamond include hydrogen [120], fluorine [121] and chlorine atoms [122]. The diamond surface is unreactive to the corresponding molecular species H_2, F_2 and Cl_2 [123]. This implies that reaction conditions necessary to generate atomic species are required. The conditions are vigorous

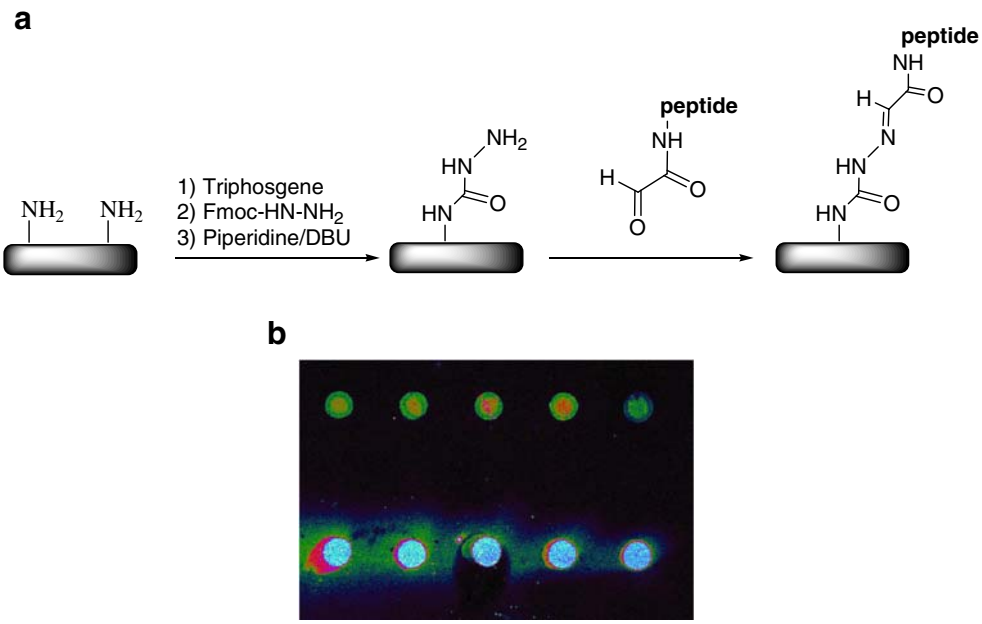

Fig. 17 **a** Formation of peptide array through site-specific α-oxo semicarbazone ligation on aminated diamond, **b** fluorescence image, *top* (peptide 1: FLAG–NH_2), *bottom* (peptide 2: FLAG–COCHO)

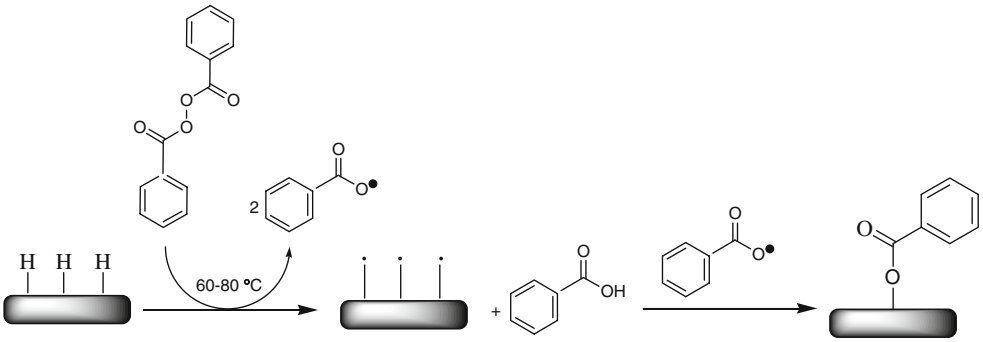

Fig. 18 Liquid phase modification of hydrogenated diamond surfaces using a radical initiator

and corrosive (e.g., Cl_2/400–500°C; F_2/470°; [42, 124]). Fluorinated diamond surfaces are stable in air and water at room temperature and have been electrochemically characterized [40, 125]. The chlorinated diamond interfaces forms hydroxylates at room temperature in contact with water vapor [126].

Milder conditions to halogenate diamond surfaces are employed when halogen atoms are formed in a photochemical reaction. The photodissociation of chlorine gas is rather well known [127]. Miller and Brown [128] prepared chlorinated polycrystalline diamond films, single crystals [123] and diamond powders [123] through the irradiation of the samples at λ =245 nm up to 24 h using a pressure Hg-arc lamp in the presence of Cl_2 gas [129].

A different photochemical approach has been used by Nakamura et al. to fluorinate H-terminated diamond surfaces [130, 131]. It is based on the photolysis of perfluoroazooctane. During this process, perfluorooctyl radicals abstract a hydrogen atom from the diamond surface. The resulting surface carbon radical reacts with another perfluorooctyl radical to yield a fluorinated surface. A similar approach has been used by Russels et al. [132], who introduced perfluorobutyl groups at low temperature on a (110)-oriented single crystal diamond surface by photolysis of a solution of perfluorobutyl iodide (C_4F_9I) using UV irradiation with a 200-W Hg-arc lamp.

There are few reports on halogenation in the liquid phase. Ikeda et al. [133] attempted chlorination of H-terminated diamond by treatment with sulfuryl chloride (SO_2Cl_2) at T=50 °C under argon atmosphere using 2,2-azobiisobutyronitrile (AIBN) as a radical initiator. The resulting chlorinated diamonds were further used for the immobilization of thymidine molecules [134]. Thymidine is a nucleoside consisting of a base combined with a sugar group in a glycosidic linkage. The DNA used was a double-stranded segment of a human phenylketonuria gene, labeled with fluorescein isothiocyanate molecules. The successful DNA binding was confirmed using confocal fluorescence microscopy. Furthermore, by comparison with transmission images, no preferential binding to certain grain boundaries was observed.

C–N bonds

The chemical reactivity of the chlorinated surface was exploited for the preparation of amine-terminated diamond. While a thermal treatment up to 450 °C in ammonia did not allow surface amination, the reaction of ammonia with chlorinated diamond was markedly different when photochemical conditions were used [123]. The chlorinated sample could be aminated by irradiation of the chlorinated diamond films in NH_3(g) at room temperature in vacuum for 3–24 h [123] or through the reaction with quaternary pyridinium salt (Fig. 15; [135]).

Reports on the direct amination of H-terminated diamond in the gas phase have only been reported recently. A radio-frequency plasma was used to promote the direct chemical reaction between the diamond surface and vaporized *N*-(6-aminohexyl)aminopropyl trimethoxysilane [136]. The relative surface density of primary amines groups ($-NH_2$) attached to the diamond surface was detected by photoluminescence, using fluorescamine in acetone spray as a fluorescence marker. On the other hand, the direct amination of hydrogen-terminated diamond surface using UV irradiation (λ=254 nm) in an ammonia gas environment was reported recently by the group of Kawarada [6, 137]. The authors have used photolithography to pattern the resulting surface and to immobilize DNA molecules in a controlled fashion. A similar approach was reported by Zhi et al. [9], where an amine functionalized boron-doped diamond surface was prepared by UV irradiation (λ=254 nm, 6 h) of a hydrogen-terminated surface in the presence of allylamine. It is believed that the vinyl groups of allylamine react photochemically with the C–H surface bonds to yield an amine-terminated monolayer covalently bonded to the surface through C–C bonds.

More recently, our group has demonstrated that the use of a cold NH_3 plasma treatment of hydrogenated diamond substrate generates surface terminal amino groups [7]. The aminated diamond surface was further investigated for its ability to bind gold nanoparticles [138] and for the formation of a peptide array [7]. As seen in Fig. 16a, homogeneous and well-distributed gold nanoparticles (Au

NPs) were obtained by simple exposure of the amine-terminated surface to an aqueous solution of gold colloid. The Au NPs modified NH_2-diamond shows interesting catalytic behavior towards oxygen reduction in basic medium (Fig. 16b), where a significant positive shift of the oxygen reduction peak and an increase in the peak current density upon loading with gold NP is observed.

The linking of glyoxylyl peptides to diamond was based on the formation of a semicarbazide termination on amine-terminated boron-doped diamond (Fig. 17a). Two different peptides (peptide 1: FLAG-NH_2 and peptide 2: FLAG-COCHO) were printed in a microarray format on semicarbazide-modified BDD. The fluorescent images (Fig. 17b), obtained after incubation in the presence of antibody anti-peptide FLAG labeled with tetramethylrhodamine shows that the fluorescence observed from peptide 2 is more important than with peptide 1. This is consistent with specific covalent ligation of peptide 2 with the semicarbazide surface and the non-covalent interaction of peptide 2 with the semicarbazide surface.

C–O bonds

Tsubota et al. [139, 140] investigated the modification of H-terminated diamond using alkyl-radicals. Among various radical initiators, benzoylperoxide was found to be the most effective in abstracting hydrogen on the surface (Fig. 18). Due to their low dissociation energy, the O–O bond in these peroxides breaks easily, generating radicals [140–148]. When benzoyl peroxide is thus heated up to temperatures of about T=60–80 °C, it decomposes into benzoyl radicals. In the presence of an H-terminated diamond surface in toluene (under argon atmosphere, at T=348 K for t=2h), the benzoyl radicals formed can abstract a hydrogen atom on the diamond surface and bind to it. Further studies using benzoyl peroxide showed that the radical reaction is highly solvent dependent. While the radical substitution reaction works well in THF and DMF, the reaction in toluene depends on the reaction conditions [142, 143]. The same group has demonstrated that aliphatic and aromatic carboxylic acids can be tethered to diamond surface through C–O bond formation by carrying out the thermal decomposition of benzoyl peroxide radical initiator in the presence of aliphatic and aromatic carboxylic acids [145, 146, 148]. In this case, R–COO° radicals are formed and bind to the diamond surface. The final chemical state of the diamond surface is determined by the kinetics of the reaction. The number of hydrogen atoms displaced on the diamond surface depends, however, strongly on the acid used. In the case of the large pyrene-carboxylic acid, rather low abstraction fraction was observed.

Conclusion

Even though diamond surfaces are chemically inert, photochemical, electrochemical and chemical approaches have shown their strength in tethering functional groups to this interface. The opportunities for diamond are wide open. To make it competitive with silicon technology, the core advantages of diamond, including the chemical stability, the low electrochemical background current and its wide potential window will have to be optimized. The control of the surface chemistry of diamond will play a crucial role in this perspective. While these interfaces are nowadays used as analytical devices in different areas, the development of new surface chemistries on diamond has somehow stagnated over the years. Two approaches to functionalize diamond interfaces have been mainly used: photochemical linking of functional alkene molecules and diazonium-based approaches. The difficulty in controlling the formation of a monolayer using diazonium-based chemistry and the immobilization of long functionalized alkene chains hindering largely electron transfer opens the search for new functionalization pathways. Some interesting approaches have been recently proposed through the direct amination of H-terminated diamond. The possibility to pattern the surface makes diamond an adapted using photopatterning to introduce functional groups inside the patterned regions makes diamond and adapted platform for the generation of microarrays. Indeed, the future application of diamond will be in high-throughput systems and biotechnologies. Whether diamond will be the material of choice for biosensing applications will depend on the effort put into the control of its surface.

References

1. Ageev VP, Chapliev NI, Konov VI, Kuzmichev AV, Pimenov SM, Ralchenko VG (1990) Phys Res 13:318
2. Matsumoto S, Sato Y, Setaka N (1981) Carbon 19:234
3. Rothschild M, Arnonr C, Ehrlich DJ (1986) J Vac Sci Technol A B4:310
4. Sappok R, Boehm HP (1968) Carbon 6:573
5. Inoue Y, Yoshimura Y, Ikeda Y, Kohno A (2000) Colloids Surf B 19:257
6. Zhang G-J, Song K-S, Nakamura Y, Ueno T, Funatsu T, Ohdomari I, Kawarada H (2006) Langmuir 22:3728–3734
7. Coffinier Y, Szunerits S, Jama C, Desmet R, Melnyk O, Marcus B, Gengembre L, Payen E, Delabouglise D, Boukherroub R (2007) Langmuir 23:4494–4497
8. Szunerits S, Jama C, Coffinier Y, Marcus B, Delabouglise D, Boukherroub R (2006) Electrochem Commun 8:1185–1190
9. Tian R-H, Rao TN, Einaga Y, Zhi J-F (2006) Chem Mater 18:939
10. Yan J-H, Song K-S, Zhang G-J, Degawa M, Sasaki Y, Ohdomari I, Kawarada H (2006) Langmuir 22:11245
11. Spitsyn BV, Bouilov LL, Derjaguin BV (1981) J Cryst Growth 52:219

12. Butler JE, Windischmann H (1998) MRS Bull 1:22
13. Sauer R (1999) Cryst Res Technol 34:227
14. Birrell J, Gerbi JE, Auciello O, Gibson JM, Johnson J, Carlisle JA (2005) Diam Relat Mater 14:86–92
15. Kulakova II (2004) Phys Solid State 46:636–43
16. Raty J-Y, Galli G (2003) Nature Mater 2:792–795
17. Wang J, Firestone MA, Auciello O, Carlisle JA (2004) Langmuir 20:11450–11456
18. Zhou D, Krauss AR, Qin LC, McCauley TG, Gruen DM, Corrigan TD, Chang RPH, Gnaser H (1997) J Appl Phys 82:4546–4550
19. Zhou D, McCauley TG, Qin LC, Krauss AR, Gruen DM (1998) J Appl Phys 83:540–543
20. Carlisle JA, Auciello O (2003) Interface 12:28
21. Gruen DM (1999) Annu Rev Mater Sci 29:211
22. Birrell J, Gerbi JE, Auciello O, Gibson J, Gruen DM, Carlisle JA (2003) J Appl Phys 93:5606
23. Bhattacharyya S, Auciello O, Birrell J, Carlisle JA, Curtis LA, Goyette AN, Gruen DM, Krauss AR, Schlueter J, Sumant A, Zapol P (2001) Appl Phys Lett 79:1441
24. Rezek B, Shin D, Nakamura Y, Nebel CE (2006) J Am Chem Soc 128:3884
25. Yang N, Uetsuka H, Watanabe H, Nakamura T, Nebel CE (2007) Chem Mater 19:2852
26. Shin D, Rezek B, Tokuda N, Takeuchi D, Watanabe H, Nakamura T, Yamamoto T, Nebel CE (2006) Phys Stat Sol (a) 13:3245
27. Ristein J, Maier F, Riedel M, Cui JB, Ley L (2000) Phys Status Solidi 181:65
28. Maier F, Riedel M, Mantel B, Ristein J, Ley L (2000) Phys Rev Lett 85:3472
29. Ri S-G, Mizumasa T, Akiba Y, Hirose Y, Kurosu T, Iida M (1995) Jpn J Appl Phys 34:5550
30. Shin D, Watanabe H, Nebel CE (2005) J Am Chem Soc 127:11237
31. Maki T, Shikama S, Komori M, Sakaguchi Y, Sakuta K, Kobayashi T (1992) Jpn J Appl Phys 31:1446
32. Albin S, Watkins L (1990) Appl Phys Lett 56:1454
33. Poferl DJ, Gardener NC, Angus JC (1973) J Appl Phys 44:1428
34. Catledge SA, Vohraa YK (1999) J Appl Phys 86:698
35. Jin S, Moustakas TD (1994) Appl Phys Lett 65:403
36. Gheeraert E, Casanova N, Tajani A, Deneuville A, Bustarret E, Garrido JA, Nebel CE, Stutzmann M (2002) Diam Relat Mater 11:289
37. Martin HB, Argoitia A, Landau U, Anderson GW, Angus JC (1996) J Electrochem Soc 143:L133
38. Swain GM, Ramesham R (1993) Anal Chem 65:345–351
39. Ferro S, De Battisti A (2003) J Phys Chem B 107:7567
40. Ferro S, De Battist A (2003) Anal Chem 75:7040–7042
41. Martin HB, Argoitia A, Angus JC, Landau U (1999) J Electrochem Soc 146:2959–2964
42. Freedman A (1994) J Appl Phys 75:3112–3120
43. Harris SJ, Belton DN (1991) App Phys Lett 57:1194
44. Kawarada H (1996) Surf Sci Rep 26:205
45. Granger MC, Swain GM (1999) J Electrochem Soc 146:4551–4558
46. Ferreira NG, Silva LLG, Corat EJ, VJ T-A (2002) Diam Relat Mater 11:1523–1531
47. Boukherroub R, Wallart X, Szunerits S, Marcus B, Bouvier P, Mermoux M (2005) Electrochem Commun 7:937–940
48. Ando T, Yamamoto K, Ishii M, Kamo M, Sato Y (1993) J Chem Soc Faraday Trans 89:3635–3640
49. Pehrsson PE, Mercer TW (2000) Surf Sci 460:49–66
50. John P, Polwart N, Troupe CE, Wilson JIB (2003) J Am Chem Soc 125:6600
51. Notsu H, Yagi I, Tatsuma T, Tryk DA, Fujishima A (1999) Electrochem Solid-State Lett 2:522
52. Yagi I, Notsu H, Kondo T, Tryk DA, Fujishima A (1999) J Electroanal Chem 473:173
53. Delabouglise D, Marcus B, Mermoux M, Bouvier P, Chane-Tune J, Petit J-P, Mailley P, Livache T (2003) Chem Comm 21:2698–2699
54. Goeting CH, Marken F, Gutiérrez-Sosa A, Compton RC (2000) Diam Relat Mat 9:390–396
55. Notsu H, Yagi I, Tatsuma T, Tryk DA, Fujishima A (2000) J Electroanal Chem 492:31–37
56. Popa E, Notsu H, Miwa T, Tryk DA, Fujishima A (1999) Electrochem Solid State Lett 2:49–51
57. Ohta R, Saito N, Inoue Y, Sugimura H, Takai O (2004) J Vac Sci Technol A 22:2005–2009
58. Boukherroub R, Wallart X, Szunerits S, Marcus B, Bouvier P, Mermoux M (2005) Electrochem Comm 7:937–940
59. Kanazawa H, Song K-S, Sakai T, Nakamura Y, Umezawa H, Tachiki M, Kawarada H (2003) Diamond Relat Mater 12:618–622
60. Riedel M, Ristein J, Ley L (2004) Diam Relat Mater 13:746–750
61. Ferro S, Battosto AD (2002) Electrochim Acta 47:1641–1649
62. Santana MHP, Faria LAD, Boodts JFC (2005) Electrochim Acta 50:2017–2027
63. Salazar-Banda G, Andrade Ls, Nascente PAP, Pinzani PS, Rocha-Filho R, Avaca LA (2006) Electrochim Acta 51:4873
64. Popa E, Notsu H, Miwa T, Tryk DA, Fujishima J (1999) Electroanal Chem 473:173
65. Fortin E, Chane-Tune J, Mailley P, Szunerits S, Marcus B, Petit J-P, Mermoux M, Vieil E (2004) Bioelectrochemistry 63:303–306
66. Foord JS, Hian LC, Jackman RB (2001) Diam Relat Mater 10:710–714
67. Foord S, Lau CH, Hiramatsu M, Jackman RB, Nebel CE, Bergonzo P (2002) Diam Relat Mater 11:856–860
68. Shirafuji J, Sugino T (1996) Diam Relat Mater 5:706–713
69. Wilson JIB, Walton JS, Beamson G (2001) J Electron Spectrosc Relat Phenom 121:183–201
70. Yamada T, Yokoyama T, Sawabe A (2002) Diam Relat Mater 11:780–783
71. Saby C, Muret P (2005) Diam Relat Mater 11:851–855
72. Boukherroub R, Szunerits S, Bouvier P, Mermeaux M (2005) Electrochem Comm
73. Notsu H, Fukazawa T, Tatsuma T, Tryk DA, Fujiwara Y (2001) Electrochem Solid-State Lett 4:H1–H3
74. Actis P, Manesse M, Nunes-Kirchner C, Wittstock G, Coffinier Y, Boukherroub R, Szunerits S (2006) Phys Chem Chem Phys 8:4924–4931
75. Bouvier P, Delabouglise D, Denoyell A, Marcus B, Mermoux M, Petit J-P (2005) Electrochem Solid-State Lett 8:E57
76. Szunerits S, Shirahata N, Actis P, Nakanishir J, Boukherroub R (2007) Chem Commun 2793
77. Delamarche E, Sundarababu G, Biebuyck H, Michel B, Gerber C, Sigrist H, Wolf H, Rigsdorf H, Xanthopoulos N, Mathieu HJ (1997) Langmuir 12:1997–2006
78. Dorman G, Prestwich GD (1994) Biochem 33:5661
79. Mazur M, Krysinski P, Blanchard GJ (2005) Langmuir 21:8802
80. Kuo T-C, McCreery RL, Swain GM (1999) Electrochem Solid State Lett 2:288–290
81. Foord JS, Hao W, Hurst S (2007) Diam Relat Mater 16:877
82. Lud SQ, Steenackers M, Jordan R, Bruno P, Gruen DM, Feulner P, Garridao JA, Stutzmann M (2006) J Am Chem Soc 128:16884
83. Matrab T, Chehimi MM, Boudou JP, Benedic F, Wang J, Naguib NN, Carlisle JA (2006) Diam Relat Mater 15:639
84. Rezek B, Shin D, Nebel CE (2007) Langmuir 23:7626
85. Shin D, Tokuda N, Rezek B, Nebel CE (2006) Electrochem Commun 8:844
86. Uetsuka H, Shin D, Tokuda N, Saeki K, Nebel CE (2007) Langmuir 23:3466
87. Wang J, Carlisle JA (2006) Diam. Rel. Mater. 15:279–284
88. Yang W, Baker SE, Butler JE, Lee C-S, Russell JN, Shang L, Sun B, Hamers RJ (2005) Chem Mater 17:938–40
89. Zhou YL, Zhi JF (2006) Electrochem Commun 8:1811

90. Allongue P, Delamar M, Desbat B, Fagebaume O, Hitmi R, Pinson J, Serveant JM (1997) J Am Chem Soc 119:201
91. Anariba F, DuVall SH, McCreery RL (2003) Anal Chem 75:3837–3844
92. Blankespoor R, Limoge B, Schnollhorn B, Syssa-Magalé J-L, Yazidi D (2005) Langmuir 21:3362
93. Brooksby PA, Downard AJ (2004) Langmuir 20:5038
94. Brooksby PA, Downard AJ (2005) J Phys Chem B 109:8791
95. Delamare M, Hitmi R, Pinson J, Savéant JM (1992) J Am Chem Soc 114:5883
96. DuVall SH, McCreery RL (2000) J Am Chem Soc 122:6759
97. Lee C-S, Baker SE, Marcus MS, Yang W, Eriksson MA, Hamers RJ (2004) Nano Lett 4:1713
98. Liu Y-C, McCreery RL (1995) J Am Chem Soc 117:11254
99. Liu Y-C, McCreery RL (1997) Anal Chem 69:2091
100. Pinson J, Podvorica F (2005) Chem Soc Rev 34:429
101. Allongue P, Delamar M, Desbat B, Fagebaume O, Hitmi R, Pinson J, Savéant J-M (1997) J Am Chem Soc 119:201
102. Hamers RJ, Butler JE, Lassetera T, Nicholsa BM, Russell JN, Tsea K-Y, Yanga W (2005) Diam Relat Mater 14:661–668
103. Rouse AA, Bernhard JB, Sosa ED, Golden DE (1999) Appl Phys Lett 75:3417
104. Strother T, Knickerbocker T, Russell JN, Butler J, Smith LM, Hamers RJ (2002) Langmuir 18:968–971
105. Knickerbocker T, Strother T, Schwartz MP, Russell JN, Butler J, Smith LM, Hamers RJ (2003) Langmuir 19:1938–1942
106. Sun B, Baker SE, Butler JE, Kim H, Russell JN, Shang L, Tse K-Y, Yang W, Hamers RJ (2007) Diam Relat Mater 16:1608
107. Lasseter TL, Clare BH, Abbott NL, Hamers RJ (2004) J Am Chem Soc 126:10220–10221
108. Yang W, Butler JE, Russell JN, Hamers RJ (2007) Analyst 132:296
109. Christiaens P, Vermeeren v, Wenmackers S, Daenen M, Haenen K, Nesladek M, vande Ven M, Ameloot M, Michiels L, Wagner P (2006) Biosens Bioelectron 22:170
110. Nebel CE, Shin D, Takeuchi D, Yamamoto T, Watanabe H, Nakamura T (2006) Diam Relat Mater 15:1107
111. Rubio-Retama J, Hernando J, Lopez-Ruiz B, Hartl A, Stinmuller D, Stutzmann M, Lopez-Cabarcos E, Garrido JA (2006) Langmuir 22:5837
112. Zhong Y-L, Chong KF, May PW, Chen Z-K, Loh KP (2007) Langmuir 23:5824
113. Yang W, Auciello O, Butler JE, Cai W, Carlisle JA, Gerbi JE, Gruen DM, Knickerbocker TL, Lasseter TL, Russell JN, Smith LM, Harmers RJ (2002) Nature Mat:253–257
114. Lu MC, Knickerbocker T, Cai W, Yang WS, Hamers RJ, Smith LM (2004) Biopolymers 73:606
115. Hartl A, Schmich E, Garrido JA, Hernanod J, Catharino SCR, Walter S, Feulber P, Kromka A, Steinmuller D, Stutzmann M (2004) Nature Mat:1–7
116. Nichols BM, Butler JE, Russell JN, Hamers RJ (2005) J Phys Chem B 109:20938
117. Nichols BM, Metz KM, Tse K-Y, Butler JE, Russell JN, Hamers RJ (2006) J Phys Chem B 110:16535
118. Strother T, Hamers RJ, Smith LM (2000) Nucleic Acids Res 28:3535
119. Yang W, Butler JE, Russell JN, Hamers RJ (2004) Langmuir 20:6778–6787
120. Yamada T, Chuang TJ, Seki H, Mitsuda Y (1991) Mol Phys 76:887
121. Freedman A, Stinespring CD (1990) AppL Phys Lett 57:1194
122. Sappok R, Boehm HP (1968) Carbon 6:283
123. Miller JB, Brown DW (1996) Langmuir 12:5809–5817
124. Liu Y, Zhenning G, Margrave JL, Khabashesku VN (2004) Chem Mat 16:3924–3930
125. Ando T, Yamamoto K, Matsuzawa M, Takamatsu Y, Kawasaki S, Okino F, Touhara H, Kamo M, Sato Y (1996) Diam Relat Mat 5:1021–1055
126. Ando T, M N-G, Rawles RE, Yamamoto K, Kamo M, Sato Y (1996) Diamond and Rel Mat 5:1136–1142
127. Gibson GE, Bayliss NS (1933) Phys Rev 44:188
128. Miller JB, Brown DW (1995) Diam Relat Mater 4:435–40
129. Miller JB (1999) Surf Sci 439:21
130. Nakamura T, Suzuki M, Ishihara M, Ohana T, Tanaka A, Koga Y (2004) Langmuir 20:5846–5849
131. Nakamura T, Tsugawa K, Ishihara M, Ohana T, Tanaka A, Koga Y (2004) Diamond and Rel Mat 13:1084–1087
132. Kim CS, Mowrey RC, Butler JE, Russell JN (1998) J Phys Chem B 102:9290–9296
133. Ikeda Y, Saito T, Kusakabe K, Morooka S, Maeda H, Taniguchi Y, Fujiwara Y (1998) Diam Relat Mater 7:830–834
134. Wenmackers S, Haenen K, Nesladek M, Wagner P, Michiels L, VandeVen M, Ameloot M (2003) Phys Stat Sol(a) 199:44–48
135. Ohtani B, Kim Y-H, Yano T, Hashimoto K, Fujishima A, Uosaki K (1998) Chem Lett 1:953–954
136. Ohta R, Saito N, Inoue Y, Sugimura H, Takai O (2004) J Vac Sci Technol A 22:2005–2009
137. Yan J-H, Song K-S, Zhang G-J, Degawa M, Sasaki Y, Ohomari I, Kawarada H (2006) Langmuir 22:11245
138. Szunerits S, Manesse M, Denault G, Marcus B, Jama C, Boukherroub R (2007) Electrochem Solid State Lett 10: G43–G6
139. Tsubota T, Urabe K, Egawa S, Takagi H, Kusakabe K, Morooka S, Meada H (2000) Diam Relat Mater 9:219
140. Tsubota T, Hirabayashi O, Ida S, Nagaoka S, Nagata M, Matsumoto Y (2002) Diam Relat Mater 11:1360–1365
141. Tsubota T, Hirabayashi O, Ida S, Nagaoka S, Nagata M, Matsumoto Y (2002) J Cer Soc Jpn 110:669–675
142. Tsubota T, Hirabayashi O, Ida S, Nagaoka S, Nagata M, Matsumoto Y (2002) Phys Chem Chem Phys 4:806–811
143. Tsubota T, Hirabayashi O, Ida S, Nagaoka S, Nagata M, Matsumoto Y (2002) Diam Relat Mater 11:1374–1378
144. Tsubota T, Ida S, Hirabayashi O, Nagaoka S, Nagata M, Matsumoto Y (2002) Phys. Chem. Chem. Phys 4:3881–3886
145. Tsubota T, Tanii S, Ida S, Nagaoka S, Matsumoto Y (2003) Phys Chem Chem Phys 5:1474–1480
146. Tsubota T, Tanii S, Ida S, Nagata M, Matsumoto Y (2004) Diam Relat Mater 13:1093–1097
147. Ida S, Tsubota T, Hirabayashi O, Nagata M, Matsumoto Y, Fujishima A (2003) Diam Relat Mater 12:601–605
148. Ida S, Tsubota T, Tanii S, Nagata M, Matsumoto Y (2003) Langmuir 19:9693–9698